Hepatic Hemorrhage Caused by Percutaneous Tumor Ablation: Radiofrequency Ablation versus Cryoablation in a Porcine Model[1]

Sarah A. Shock, MD[2]
Paul F. Laeseke, BS
Lisa A. Sampson, CVT
William D. Lewis, MD
Thomas C. Winter III, MD
Jason P. Fine, ScD
Fred T. Lee, Jr, MD

Published online
10.1148/radiol.2361040533
Radiology 2005; 236:125–131

Abbreviations:
ANOVA = analysis of variance
RF = radiofrequency

[1] From the Departments of Radiology (S.A.S., P.F.L., L.A.S., W.D.L., T.C.W., F.T.L.) and Biostatistics and Medical Informatics (J.P.F.), University of Wisconsin Hospital and Clinics, 600 Highland Ave, Madison, WI 53792-3252. Supported in part by Endocare, Irvine, Calif. Received March 22, 2004; revision requested June 2; revision received July 14; accepted August 18. **Address correspondence to** F.T.L. (e-mail: *ftlee@wisc.edu*).

Current address:
[2] Department of Radiology, New York University, New York, NY.

Author contributions:
Guarantor of integrity of entire study, F.T.L.; study concepts and design, S.A.S., F.T.L.; literature research, L.A.S., S.A.S., P.F.L., F.T.L.; experimental studies, S.A.S., P.F.L., L.A.S., W.D.L., T.C.W., F.T.L.; data acquisition, S.A.S., P.F.L., L.A.S.; data analysis/interpretation, S.A.S., P.F.L., L.A.S., J.P.F.; statistical analysis, J.P.F.; manuscript preparation, S.A.S., P.F.L., L.A.S., F.T.L.; manuscript definition of intellectual content, S.A.S., P.F.L., F.T.L.; manuscript editing, P.F.L., F.T.L.; manuscript revision/review, all authors; manuscript final version approval, S.A.S., P.F.L., J.P.F., T.C.W., L.A.S., F.T.L.

PURPOSE: To determine the extent of hepatic hemorrhage caused by percutaneous cryoablation performed with a small-diameter cryoablation probe compared with that caused by percutaneous radiofrequency (RF) ablation in a porcine model.

MATERIALS AND METHODS: The study was preapproved by the institutional research animal care and use committee, and husbandry and experiments complied with National Institutes of Health standards for care and use of laboratory animals. Percutaneous hepatic ablation was performed in 18 domestic pigs (mean weight, 45 kg) by using a 17-gauge (1.5-mm-diameter) RF electrode ($n = 6$), a cluster of three RF electrodes ($n = 6$), or a 13-gauge (2.4 mm-diameter) cryoprobe ($n = 6$). Ablation was performed in four sites per liver. Total blood loss, minimum lesion diameter, maximum lesion diameter, and lesion volume were determined for each group and compared by using analysis of variance.

RESULTS: Mean blood loss was 11.11 mL ± 11.47 (standard deviation), 105.29 mL ± 175.58, and 28.06 mL ± 30.97 with the single RF electrode, RF electrode cluster, and cryoablation probe, respectively. Mean minimum and maximum lesion diameters were largest with the RF electrode cluster (2.40 and 3.98 cm, respectively), followed by the cryoablation probe (2.38 and 3.94 cm) and single RF electrode (1.49 and 2.63 cm). Mean minimum and maximum lesion diameters were significantly different between the single RF electrode and the RF electrode cluster, as well as between the single RF electrode and the cryoablation probe ($P < .001$). Mean lesion volume was largest for the RF electrode cluster (24.03 cm^3), followed by those for the cryoablation probe (17.46 cm^3) and single RF electrode (9.05 cm^3) (single RF electrode vs cryoablation probe, $P < .05$). Lesion volumes were not significantly different with the RF electrode cluster versus the single RF electrode ($P = .052$) or with the RF electrode cluster versus the cryoablation probe ($P = .381$).

CONCLUSION: Mean blood loss from percutaneous cryoablation in this model was between that for RF ablation with the single electrode and that for RF ablation with the electrode cluster.

Surgical resection is considered the standard treatment for primary and metastatic liver cancer. Unfortunately, only 5%–10% of patients have tumors suitable for surgical removal, because of lesion location and/or number or associated comorbidities (1,2). A desire to provide minimally invasive treatments for patients with unresectable malignancies has driven research into focal tumor ablation technologies, primarily those of radiofrequency (RF) ablation and cryoablation. In RF ablation, an alternating electrical current is used to create ionic agitation, which produces frictional heat and subsequent tissue necrosis (3). Cryoablation produces rapid freezing of tissue, with resultant cell death due to ice crystallization, desiccation, ischemia, and reperfusion injury during thawing (4). Several recent studies have shown that both of these techniques are effective treatment modalities for local control of selected tumors with low complication rates (5–10).

RF ablation is performed by using small applicators (14–17 gauge), and the heat produced during RF application results in electrocautery. These factors have led to the rapid acceptance of RF for percutaneous treatment of tumors of the liver, kidney, bone, and lung (11–14). Bleeding rates are very low when RF ablation is combined with tract cautery after probe removal (15,16). In fact, several studies have demonstrated the potential of RF energy for use in preventing postbiopsy bleeding (17,18).

Cryoablation has long been recognized as an important adjunct to surgical resection, but it has mainly been applied at open or laparoscopic surgery rather than percutaneously. This lack of percutaneous use is due to the need for large probes with an outer diameter of 3–8 mm (11–0 gauge) and the belief that direct surgical inspection is needed to monitor for complications such as liver cracking, which may cause severe hemorrhage (10,19–22). While the overall morbidity and mortality of cryoablation are low, researchers in a large-scale study reported that 12% of mortality and 17% of morbidity associated with hepatic cryoablation were due to hemorrhage (23). Investigators in studies of open surgical cryoablation in which large cryoprobes (3–8 mm in diameter) were placed by using the Seldinger technique and in which slow-cooling nitrogen-based systems were used have cited liver cracking and hemorrhage as a serious complication (21,23). Researchers in preliminary studies of percutaneous cryoablation, however, have not reported hepatic hemorrhage (24–26). The lack of hemorrhage may be due to the use of newer 2.4-mm trocar-tipped cryoprobes designed specifically for percutaneous use and to rapid-cooling argon-based cryoablation systems. The ability to safely use percutaneous cryoablation would allow physicians and patients to realize some of the unique benefits of cryoablation applied in a minimally invasive fashion. Thus, the purpose of our study was to determine the extent of hepatic hemorrhage caused by percutaneous cryoablation performed with small-diameter cryoprobes compared with that caused by percutaneous RF ablation in a porcine model.

MATERIALS AND METHODS

Animals, Anesthesia, and Procedures

Twenty healthy female domestic swine (mean weight, 45 kg) were used for this study. Preapproval was obtained from the research animal care and use committee of our institution, and all husbandry and experimental studies were compliant with the National Institutes of Health guidelines for the care and use of laboratory animals (*www.nap.edu/readingroom/books/labrats/*). Anesthetic induction was achieved with 320 mg intramuscular tiletamine hydrochloride and zolazepam hydrochloride (Telazol; Fort Dodge Animal Health, Fort Dodge, Iowa), 0.54 mg atropine (Phoenix Pharmaceutical, St Joseph, Mo), and 100 mg xylazine hydrochloride (Xyla-Ject; Phoenix Pharmaceutical). Animals were intubated, and anesthesia was maintained with 1.5%–2.5% inhaled isoflurane (Halocarbon Laboratories, River Edge, NJ). Postprocedural pain control was achieved with an intramuscular injection of 0.9 mg buprenorphine (Reckitt Benckiser, Richmond, Va). A second dose of intramuscular buprenorphine was administered 6 hours after the initial dose. The abdomen was shaved, scrubbed with 2% chloroxylenol, and prepared with a 10% povidone-iodine solution. All pigs received 500 mL of intravenous lactated Ringer solution during the procedures. Puncture sites were closed with tissue adhesive (VetBond; 3M, St Paul, Minn). Hematocrit and hemoglobin levels were measured for each pig prior to the start of RF ablation or cryoablation and just prior to sacrifice 24 hours later.

Two pigs in the single-electrode RF ablation group had respiratory symptoms and frothy pink respiratory secretions that were noticed during intubation prior to the experimental procedures. Both animals expired of respiratory compromise during recovery from anesthesia. Necropsy by the institutional veterinary group confirmed hemorrhagic pneumonia as the cause of death. These pigs were subsequently excluded from the study. The animal vendor was changed following the death of the second animal, and the remaining 13 pigs were given a prophylactic intramuscular injection of 200 mg enrofloxacin (Baytril; Bayer, Shawnee Mission, Kan) 3 days prior to the procedure and on the day of the procedure. After these changes, no further respiratory or other complications were encountered during the remainder of the study.

Experimental Groups

No data were obtained from the two animals that expired from pneumonia. As a result, a total of 20 animals were used for this study, but only 18 pigs (six per group) constituted the study sample. Group 1 consisted of animals treated with single-electrode RF ablation, group 2 consisted of animals treated with clustered-electrode RF ablation, and group 3 consisted of animals treated with percutaneous cryoablation.

Ultrasonographic Equipment and Guidance during Applicator Placement

Real-time ultrasonographic (US) guidance was used for all applicator placements described in this study (Sonoline Antares MSC 2704 AB; Siemens, Issaquah, Wash). A single RF electrode, a cluster of three RF electrodes, or a cryoablation probe was percutaneously advanced into the liver after an adequate target area was selected. An attempt was made to place one applicator in each of the four lobes of the liver (right lateral, right medial, left lateral, and left medial) by one or more of several authors (S.A.S., P.F.L., L.A.S., W.D.L., F.T.L.). Thus, four lesions were created in each porcine liver. An attempt was made to place the applicator in the center of each hepatic lobe and to avoid thermal injury to the colon or stomach. The number of punctures through the liver capsule was recorded. During RF ablation, thermal lesions were created consecutively after all four electrodes were placed. During cryoablation, ice balls were created simultaneously after placement of all four probes.

RF Ablation

All RF procedures in this study were performed by using either a single electrode (Cool-tip; Valleylab, Boulder, Colo) or a three-electrode cluster (Cool-tip Cluster; Valleylab). The electrodes we used are 17 gauge (1.5 mm in diameter). In the single electrode, the shaft is insulated, with the exception of a 3.0-cm length of exposed tip (Fig 1a). The RF electrode cluster consists of three electrodes fixed in a triangular configuration with 5 mm of separation. Each electrode in the cluster is identical to the single RF electrode except in regard to the length of the exposed tip, which is 2.5 cm for electrodes in the cluster (Fig 1b). We used a 480-kHz monopolar RF generator (Cool-tip RF Ablation System; Valleylab) that operates at

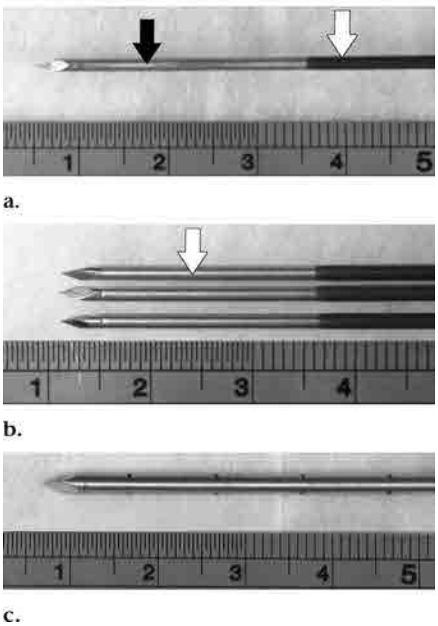

Figure 1. Photographs show (a) the single RF electrode, a 17-gauge cooled-tip probe with insulated shaft (white arrow) and 3.0-cm uninsulated active distal tip (black arrow); (b) the RF electrode cluster, three single electrodes fixed in triangular configuration at 5 mm of separation, each electrode identical to the single RF electrode but with a shorter (2.5-cm) exposed tip (arrow); and (c) the cryoprobe, a straight 2.4-mm-diameter (13-gauge) cutting-tip percutaneous probe 15 cm long, with a 3.6-cm uninsulated tip cooled by highly pressurized argon gas.

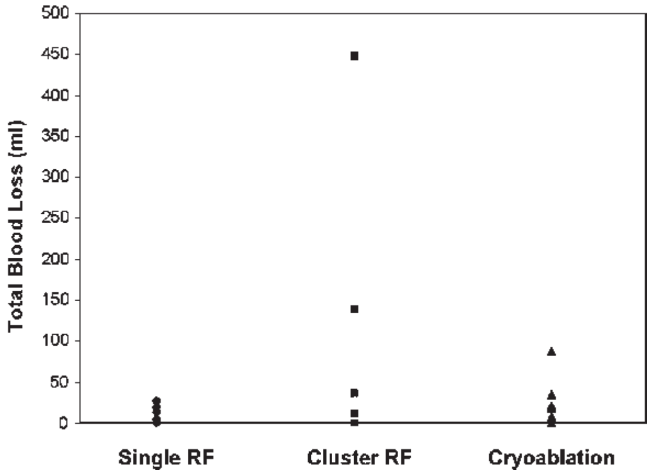

Figure 2. Graph shows total blood loss (in milliliters) for each animal in the ablation groups. Note that one animal in the clustered-electrode RF ablation group experienced a blood loss much greater than the others in that group.

a maximum of 200 W (2.0 A at 50 Ω). When the generator is operated in automatic mode, during ablation, output is controlled by an algorithm with an impedance feedback loop that is used to maximize energy delivery by minimizing charring. RF energy was applied for a total of 12 minutes per lesion, according to the manufacturer's recommendations (27). An infusion pump (Cool-tip RF System PE-PM; Valleylab) was used to circulate chilled sterile water (approximately 18°–20°C at the electrode tip) through the electrodes during ablation, to limit tissue charring. Electrocautery of the tract was performed during withdrawal of the electrodes by operating the generator in manual mode with a target temperature of 70°C. When this temperature was achieved, the electrode was slowly withdrawn until the tip temperature decreased to less than 70°C, at which time the electrode was held stationary. Cautery was performed in this fashion until the electrode was just below the skin surface at the liver capsule.

Cryoablation

The cryoablation unit used for this study was an argon gas–based system (Cryocare; Endocare, Irvine, Calif). Cryoablation was performed by one or more authors (S.A.S., P.F.L., L.A.S., W.D.L., F.T.L.) using straight 2.4-mm-diameter (13-gauge) sharp-tip percutaneous cryoprobes, 15 cm in length, with 3.6 cm of uninsulated probe at the tip. Figure 1c shows the tip of one of the cryoprobes. The cooling of cryoprobes with argon gas, based on the Joule-Thompson effect, occurs when the pressurized gas is pumped into an expansion chamber at the probe tip (28). The argon gas used as a cryogen in this system is pressurized to a minimum of 3000 psi. Helium gas, which is used for thawing, is pressurized to a minimum of 900 psi. For this study, a double-freeze clinical protocol was used, with a 10-minute freeze followed by a 5-minute passive thaw and then a second 10-minute freeze followed by an active thaw to allow the probe to be withdrawn (7).

Animal Sacrifice

The day after RF ablation or cryoablation, the pigs were again anesthetized, and hematocrit and hemoglobin levels were measured. A midline abdominal incision was then performed for peritoneal exploration and liver exposure. Care was taken not to spill blood into the peritoneal cavity during laparotomy. Any clots seen on the liver surface or in the abdomen or pelvis were removed and weighed. Most of the peritoneal fluid was suctioned from the peritoneal cavity, and the volume was recorded. The hematocrit level (in percentage) was obtained with testing of a sample of this peritoneal fluid. Any remaining peritoneal fluid was removed with laparotomy pads that were weighed and then placed in the abdominal cavity. The pads were weighed again after the fluid was absorbed, and the total volume of the peritoneal fluid was calculated. The animal was then sacrificed with an intravenous overdose (1 mL/45.4 kg) of pentobarbital sodium (390 mg/mL) and phenytoin sodium (50 mg/mL) (Beuthanasia-D; Schering-Plough, Kenilworth, NJ). The liver was removed en bloc, placed in formalin for a minimum of 24 hours, and sectioned at 3-mm intervals.

Blood Loss Determination

Blood loss was estimated in milliliters by using the formula $BL = BL_C + BL_{PF}$, where BL is the total amount of blood lost during or after the procedure, BL_C is the amount of blood loss determined from clots found in the peritoneal cavity, and BL_{PF} is the amount of blood in the peritoneal fluid.

The amount of blood loss determined from the clots was calculated as follows: $BL_C = V_C/Hct_{pre}$, where V_C is the volume of the clots (in milliliters) found on the liver surface or in the peritoneal cavity and Hct_{pre} is the preprocedural hematocrit level. Because a clot represents only the cellular portion of blood, the amount of whole-blood loss was calculated by dividing the clot weight by the preproce-

TABLE 1
Blood Loss in Porcine Model of Tumor Ablation

Variable and ANOVA Result	Clot Blood Loss	Peritoneal Fluid Blood Loss	Total Blood Loss
Applicator type			
Single RF electrode	9.97 (10.58)*	1.13 (1.50)†	11.11 (11.47)‡
RF electrode cluster	93.07 (154.59)§	12.21 (21.04)‖	105.29 (175.58)#
Cryoablation probe	18.76 (23.42)	9.30 (8.05)	28.06 (30.97)
P value	.25	.34	.27

Note.—Unless otherwise indicated, data are mean volumes measured in milliliters in 18 pigs after ablation performed with one of three applicators (each applicator was used in six pigs). Data in parentheses are standard deviations.
* $P = .22$ for comparison with electrode cluster and $P = .42$ for comparison with cryoablation probe.
† $P = .23$ for comparison with electrode cluster and $P = .035$ for comparison with cryoablation probe.
‡ $P = .22$ for comparison with electrode cluster and $P = .24$ for comparison with cryoablation probe.
§ $P = .27$ for comparison with cryoablation probe.
‖ $P = .76$ for comparison with cryoablation probe.
\# $P = .31$ for comparison with cryoablation probe.

TABLE 2
Lesion Diameter and Volume after Ablation

Variable and ANOVA Result	Minimum Diameter (cm)	Maximum Diameter (cm)	Lesion Volume (cm^3)
Applicator type			
Single RF electrode	1.49 (0.58)*	2.63 (0.82)*	9.05 (4.16)†
RF electrode cluster	2.40 (1.07)‡	3.98 (0.69)§	24.03 (16.16)‖
Cryoablation probe	2.38 (0.69)	3.94 (0.95)	17.46 (6.92)
P value	<.001	<.001	.074

Note.—Unless otherwise indicated, data are means. Data in parentheses are standard deviations.
* $P < .001$ both for comparison with electrode cluster and for that with cryoablation probe.
† $P = .05$ for comparison with electrode cluster and $P = .03$ for that with cryoablation probe.
‡ $P = .94$ for comparison with cryoablation probe.
§ $P = .87$ for comparison with electrode cluster.
‖ $P = .38$ for comparison with cryoablation probe.

dural hematocrit level. Clot weight in this study was assumed to approximate clot volume.

The amount of blood in the peritoneal fluid was calculated by using the formula $BL_{PF} = (Hct_{PF}/Hct_B) \cdot V_{PF}$, where Hct_{PF} is the hematocrit level in the peritoneal fluid, Hct_B is the baseline hematocrit level, and V_{PF} is the volume of fluid in the peritoneal cavity (in milliliters). The hematocrit level in the peritoneal fluid was divided by the baseline hematocrit level to determine the concentration of blood in the peritoneal fluid. The quotient was multiplied by the total volume of fluid in the peritoneal cavity to obtain the total amount of blood in the peritoneal fluid. The volume of the peritoneal fluid was calculated by adding the volume of fluid suctioned from the peritoneal cavity to the volume of fluid absorbed by the laparotomy pads.

Lesion Volume and Diameter Determination

Liver slices were placed directly on an optical scanner (Perfection 2450 Photo; Epson, Long Beach, Calif), and images were saved electronically as digital files. The lesion size was analyzed by using Java-based image processing and analysis freeware (Image J; available at *rsb.info.nih.gov/ij*). Lesion measurements were performed by using the central pale zone of complete necrosis for RF ablation and the entire red zone of necrosis for cryoablation. These zones previously were shown to correspond to the area of complete cell necrosis (29–33). If zones of thermal ablation crossed lobes, the entire zone of ablation was measured. The minimum and maximum diameters were measured by one of two authors (S.A.S., P.F.L.). The total volume per lesion (V_{tot}) was calculated by multiplying the area for each lesion by the slice thickness and then summing the volumes of all the slices: $V_{tot} = (A_1 \cdot T) + (A_2 \cdot T) + \cdots + (A_n \cdot T)$, where A is the area of each slice, T is the slice thickness, and n is the ordinal number of the slice (29). The total volume of tissue ablated per pig also was calculated.

Statistical Analysis

Single-electrode RF ablation, clustered-electrode RF ablation, and cryoablation were compared with respect to blood loss in clots, blood loss in peritoneal fluid, and total blood loss by using the F test with the variance ratio obtained from analysis of variance (ANOVA). Two-sample Student t tests were performed to see whether the results were different from those obtained with ANOVA. ANOVA was used to test differences in mean lesion minimum diameter, mean lesion maximum diameter, and mean lesion volume across the different ablation techniques. Statistical significance was defined by $P < .05$. Calculations were performed by using software (S-Plus, version 3.4 [1996]; MathSoft, Cambridge, Mass).

RESULTS

Applicator Placements

The total number of probe placements was identical for each group. One animal in each group required the re-placement of one probe. Therefore, the total number of liver capsule punctures in each group was 25, or 4.2 per pig.

Blood Loss Comparison

Total blood loss plotted for each animal is shown in Figure 2. Means (± standard deviations) for blood loss measurements in each group are given in Table 1. The P values for all paired-data comparisons, obtained by using two-sample Student t tests, are also listed in Table 1. In summary, blood loss was least for single-electrode RF ablation (11.1 mL ± 11.5), followed by cryoablation (28.1 mL ± 31.0) and clustered-electrode RF ablation (105.3 mL ± 175.6). The difference between the volume of blood loss in peritoneal fluid at single-electrode RF ablation and that at cryoablation was marginally significant ($P = .035$). There were no other statistically significant differences in blood loss between groups ($P > .05$).

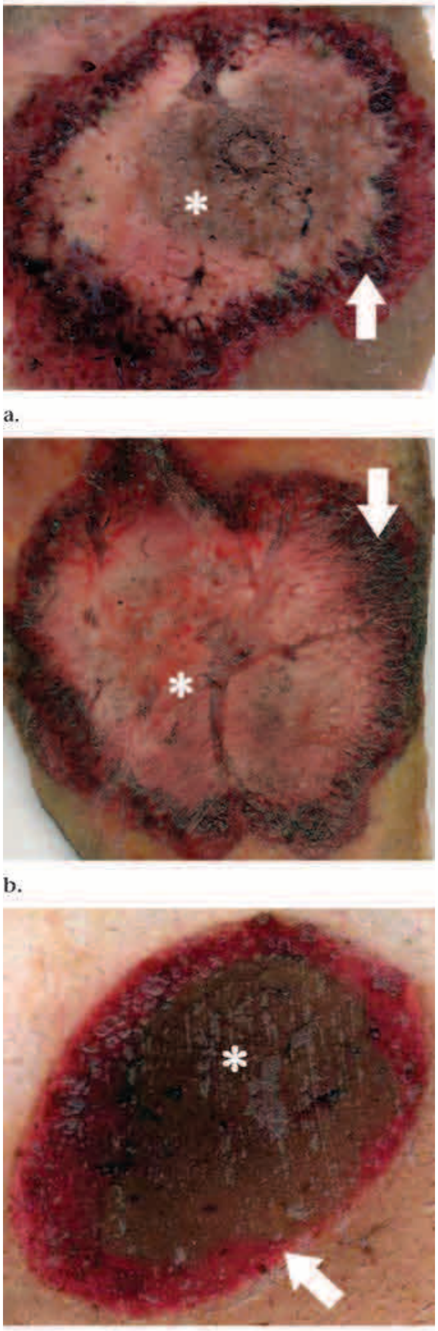

a.

b.

c.

Figure 3. Thermal lesions from RF ablation with **(a)** the single electrode and **(b)** the electrode cluster both have a characteristic inner pale zone of complete necrosis (*) and outer red and black zone of hemorrhage, congestion, and partial necrosis (arrow), but lesion in **b** (2.5-cm minimum diameter, 3.3-cm maximum diameter) is larger than that in **a** (1.9-cm minimum diameter, 2.6-cm maximum diameter). **(c)** Lesion from cryoablation (2.3-cm minimum diameter, 3.5-cm maximum diameter) differs markedly in appearance from **a** and **b**, with oval shape and with brownish-black necrotic center (*) bordered by thin pale rim (arrow) that corresponds to infiltration by leukocytes. Note precise demarcation between necrotic zone and normal hepatic tissue.

TABLE 3
Hematocrit Levels before and after Ablation

Variable and ANOVA Result	Preprocedural Hematocrit Level (%)	Postprocedural Hematocrit Level (%)
Applicator type		
Single RF electrode	24.33 (2.16)	24.50 (6.50)
RF electrode cluster	25.83 (3.43)	27.16 (6.55)
Cryoablation probe	24.00 (3.84)	26.16 (5.11)
P value	.55	.75

Note.—Unless otherwise indicated, data are means. Data in parentheses are standard deviations.

Lesion Diameter and Volume Comparison

Lesion diameters and lesion volumes are listed in Table 2. Clustered-electrode RF ablation produced the largest mean lesion minimum diameter, as well as the largest lesion maximum diameter and volume, followed by cryoablation and single-electrode RF ablation. The differences in minimum and maximum lesion diameter for single-electrode RF ablation versus clustered-electrode RF ablation or cryoablation were significant, while those for clustered-electrode RF ablation versus cryoablation were not. The difference in lesion volume for single-electrode RF ablation versus cryoablation was significant, while those for clustered-electrode RF ablation versus cryoablation and for single-electrode RF ablation versus clustered-electrode RF ablation were not. Results of paired *t* tests for differences in lesion measurements are listed in Table 2.

Gross Pathologic Examination

Figure 3 shows examples of lesions created by using each of the three ablation modalities. Lesions from RF ablation are characterized by an inner pale zone and an outer red zone: The pale zone corresponds to the region of necrosis, while the red zone contains hemorrhage, congestion, and partial necrosis of hepatocytes (30). The lesion from cryoablation is a deep-red oval zone bordered by a thin white rim of tissue that corresponds to the zone of infiltration by leukocytes (31).

Hematocrit Levels

Pre- and postprocedural hematocrit levels are shown in Table 3. No significant differences in hematocrit levels were noted either between ablation groups or between pre- and postprocedural measurement times.

DISCUSSION

Both RF ablation and cryoablation have been used to successfully treat liver tumors, but cryoablation generally has been confined to use during conventional open surgery or laparoscopy because of fears of uncontrolled hepatic hemorrhage. These fears arose after the publication of several reports of post-cryoablation hemorrhage early in the development of the technique (21,23). In contrast, recent limited clinical experience with percutaneous cryoablation of the liver, lung, and kidney has not been associated with substantial hemorrhage (24–26,34). In addition, the results of our study demonstrate no significant difference in blood loss between percutaneous RF ablation with an electrode cluster and cryoablation in a porcine model. There are several potential explanations for the conflicting results between early and more recent experience with cryoablation-associated hemorrhage. The first is that the body wall may effectively tamponade the puncture sites created with both RF ablation and cryoablation. It is also possible that the hemorrhage encountered in historic studies of cryoablation was associated with hepatic cracking due to freezing in a very large volume. While it is possible that some physicians will still treat very large tumors with ablation, reports of increased local failures and complications associated with ablation in large tumors have discouraged many physicians from routinely treating large tumors with ablation of any modality (35,36).

Cryoablation has several potential advantages over RF ablation for the destruction of liver tumors. Although all focal thermal ablation techniques are limited by vascularly mediated cooling (or heating), which may preserve perivascular tumor cells (37,38), there is some evidence that cryoablation is more likely to overcome this effect without vascular occlusion due to the extreme cold (approximately −150°C) produced by modern argon gas–based systems (32). An additional advantage of cryoablation is the ability to simultaneously use multiple cryoprobes. The use of multiple probes is thermally synergistic, and several probes placed simultaneously in close proximity create a much colder thermal environment than do consecutive placements of a single probe (39). Finally, unlike thermal lesions created during RF ablation, the ball of ice created during cryoablation is easily visualized and monitored with US, computed tomography, and magnetic resonance imaging (31,40–42).

In our study, the amount of bleeding created by percutaneous cryoablation ranged between those created by single-electrode RF ablation and by clustered-electrode RF ablation. Both RF electrode configurations are widely accepted as safe for human use, and both have been extensively used around the world with low complication rates (6). The new design of percutaneous cryoprobes (cutting tip), the trocar method of probe placement, and the tamponade effect produced by the body wall also likely contribute to the low rates of bleeding seen in our study. In most early studies of cryoablation, blunt cryoprobes were placed by using the Seldinger technique, which requires progressive tract dilation and placement of a blunt probe through a sheath with a larger diameter than that of the probe. In terms of the surface area of the hole that was created in the liver capsule by the different applicators in our study, the 2.4-mm percutaneous cryoprobe created a hole that was larger (0.045 cm^2) than that with the single 17-gauge RF electrode (0.017 cm^2) but smaller than the conglomerate hole created by the electrode cluster (0.051 cm^2). In contrast, the surface area of the 11-F sheath (0.11 cm^2) typically used for placement of 3.0-mm cryoablation probes in early studies is much larger than those of the applicators used at RF ablation or cryoablation. Perhaps the amount of bleeding in the percutaneous environment is best correlated with the size of the hole created in the liver capsule (or the increased number of punctures, in the case of the electrode cluster), regardless of the type of applicator. An additional factor should be considered that pertains to the RF electrode cluster. Ideally, the prongs of this device are placed at the skin surface in an equilateral triangle through a guide and are inserted straight into a tumor. Once the probe has penetrated the skin, however, the prong tips are no longer fixed in position relative to each other, and the tips may spread apart or become bunched. Because the prongs are fixed in the handle, forward pressure may create shear forces that could cause tissue trauma out of proportion to the size of the puncture hole. Indeed, in our study, the two largest amounts of blood loss (447.61 and 137.43 mL) were associated with use of the electrode cluster. Reanalysis of the data with the exclusion of the animal that bled 447.61 mL did not substantially change the statistical result; as expected, however, removal of the outlier decreased the difference between groups and strengthened the conclusion that the difference was not significant.

It is possible that the amount of blood loss associated with RF ablation procedures in our study and in clinical cases could be decreased with the use of higher temperatures during tract cautery. To our knowledge, however, there is no evidence in the literature that a systematic study of this question has taken place. We therefore elected to use the manufacturer-recommended target temperature of 70°C. If tract cautery is performed at higher temperatures, the risk of skin burns may increase if the operator withdraws the RF electrode into the subcutaneous tissues and skin during heating. Cryoablation lacks an intrinsic cautery effect. Therefore, to achieve further decreases in blood loss with cryoablation, the use of smaller applicators or coaxial technique and tract embolization will likely be required.

The formula used to calculate total blood loss in our study was derived from the fact that hepatic bleeding may be manifested both as clots adherent to the liver capsule and as intraperitoneal hemorrhage. Since a clot is largely devoid of serum, the amount of whole blood that resulted in the measured clot was calculated by using the pig's hematocrit level as the reference standard. Since pigs normally have ascites, we were able to determine the approximate amount of whole blood in the ascitic fluid also by comparing the hematocrit level of the blood with that of the ascitic fluid. The combination of these values resulted in the total blood loss value. While this formula probably reflects blood loss more accurately than does clot weight, the results of our study would have been unchanged if clot weight were the only measure used for blood loss. For all techniques, the amount of blood loss was relatively small and likely to be clinically insignificant. The normal circulating blood volume is approximately 2.9 L in a 45-kg pig (43). The mean blood loss at single-electrode RF ablation, cryoablation, and clustered-electrode RF ablation was 0.38%, 0.97%, and 3.63%, respectively, of this total circulating blood volume. As a rough guide, up to 10% of a pig's total circulating blood volume can be collected at any time, with minimal adverse effects (43). The mean blood losses seen in our study were well below this level and therefore were unlikely to be clinically significant.

Hematocrit levels were measured immediately prior to ablation and 24 hours after the procedure. The small increase in postprocedural hematocrit level was likely a result of dehydration due to either insufficient intraprocedural hydration (constant at 500 mL lactated Ringer solution) or a lack of oral hydration by the pigs during recovery from anesthesia and ablation. No decrease in the hematocrit level was seen in any group, regardless of the ablation technique.

The greatest limitation of our study was the use of a normal porcine liver model. Pigs are a commonly used model for ablation studies (44–46) and have been used in the past to measure blood loss for percutaneous image-guided procedures (18). There is no appropriate large-animal model of liver tumors that is ideal for use with human RF electrodes or cryoablation probes, and large-animal models of cirrhosis are complex and costly. The anatomy of the porcine liver, compared with that of the human liver, makes it somewhat more susceptible to ablation-related bleeding, because of its flat, overlapping, multilobed configuration. The porcine liver anatomy results in an increased number of opportunities for the applicator to cross the hepatic capsule. Since bleeding between lobes can lead to intraperitoneal hemorrhage, it is possible that our use of the porcine model may have resulted in an overestimation of the amount of bleeding that would occur in a normal (noncirrhotic) human liver. In this study, the relative risk of hemorrhage in subjects with coagulopathy or portal hypertension also was not assessed. It is possible that the cautery effect of RF ablation may give it an advantage over cryoablation for use in such patients.

Practical application: Both percutaneous cryoablation and percutaneous RF ablation were safely applied in a porcine model, without evidence of substantial hemorrhage. Recent development of small-diameter cryoprobes and argon-based cryoablation systems may allow more patients to realize the unique ben-

Radiology

efits of cryoablation applied in a minimally invasive fashion.

Acknowledgment: The authors are grateful to Carrie E. Poole for general assistance in manuscript preparation.

References

1. Ravikumar TS, Steele GD Jr. Hepatic cryosurgery. Surg Clin North Am 1989; 69:433–440.
2. Nagorney DM, Gigot JF. Primary epithelial hepatic malignancies: etiology, epidemiology, and outcome after subtotal and total hepatic resection. Surg Oncol Clin N Am 1996; 5:283–300.
3. Organ LW. Electrophysiologic principles of radiofrequency lesion making. Appl Neurophysiol 1976–1977; 39:69–76.
4. Shafir M, Shapiro R, Sung M, Warner R, Sicular A, Klipfel A. Cryoablation of unresectable malignant liver tumors. Am J Surg 1996; 171:27–31.
5. Solbiati L, Livraghi T, Goldberg SN, et al. Percutaneous radio-frequency ablation of hepatic metastases from colorectal cancer: long-term results in 117 patients. Radiology 2001; 221:159–166.
6. Livraghi T, Solbiati L, Meloni MF, Gazelle GS, Halpern EF, Goldberg SN. Treatment of focal liver tumors with percutaneous radio-frequency ablation: complications encountered in a multicenter study. Radiology 2003; 226:441–451.
7. Cha C, Lee FT Jr, Rikkers LF, Niederhuber JE, Nguyen BT, Mahvi DM. Rationale for the combination of cryoablation with surgical resection of hepatic tumors. J Gastrointest Surg 2001; 5:206–213.
8. Ravikumar TS, Steele G Jr, Kane R, King V. Experimental and clinical observations on hepatic cryosurgery for colorectal metastases. Cancer Res 1991; 51:6323–6327.
9. Yeh KA, Fortunato L, Hoffman JP, Eisenberg BL. Cryosurgical ablation of hepatic metastases from colorectal carcinomas. Am Surg 1997; 63:63–68.
10. Weaver ML, Atkinson D, Zemel R. Hepatic cryosurgery in the treatment of unresectable metastases. Surg Oncol 1995; 4:231–236.
11. McGahan JP, Dodd GD 3rd. Radiofrequency ablation of the liver: current status. AJR Am J Roentgenol 2001; 176:3–16.
12. Gervais DA, McGovern FJ, Arellano RS, McDougal WS, Mueller PR. Renal cell carcinoma: clinical experience and technical success with radio-frequency ablation of 42 tumors. Radiology 2003; 226:417–424.
13. Dupuy DE, Zagoria RJ, Akerley W, Mayo-Smith WW, Kavanagh PV, Safran H. Percutaneous radiofrequency ablation of malignancies in the lung. AJR Am J Roentgenol 2000; 174:57–59.
14. Rosenthal DI, Hornicek FJ, Torriani M, Gebhardt MC, Mankin HJ. Osteoid osteoma: percutaneous treatment with radiofrequency energy. Radiology 2003; 229:171–175.
15. Rhim H, Dodd GD 3rd. Radiofrequency thermal ablation of liver tumors. J Clin Ultrasound 1999; 27:221–229.
16. Chung MH, Wood TF, Tsioulias GJ, Rose DM, Bilchik AJ. Laparoscopic radiofrequency ablation of unresectable hepatic malignancies: a phase 2 trial. Surg Endosc 2001; 15:1020–1026.
17. Pritchard WF, Wray-Cahen D, Karanian JW, Hilbert S, Wood BJ. Radiofrequency cauterization with biopsy introducer needle. J Vasc Interv Radiol 2004; 15:183–187.
18. Laeseke PF, Winter TC 3rd, Davis CL, et al. Postbiopsy bleeding in a porcine model: reduction with radio-frequency ablation—preliminary results. Radiology 2003; 227:493–499.
19. Seifert JK, Junginger T, Morris DL. A collective review of the world literature on hepatic cryotherapy. J R Coll Surg Edinb 1998; 43:141–154.
20. Wong WS, Patel SC, Cruz FS, Gala KV, Turner AF. Cryosurgery as a treatment for advanced stage hepatocellular carcinoma: results, complications, and alcohol ablation. Cancer 1998; 82:1268–1278.
21. Onik GM, Atkinson D, Zemel R, Weaver ML. Cryosurgery of liver cancer. Semin Surg Oncol 1993; 9:309–317.
22. Pearson AS, Izzo F, Fleming RY, et al. Intraoperative radiofrequency ablation or cryoablation for hepatic malignancies. Am J Surg 1999; 178:592–599.
23. Seifert JK, Morris DL. World survey on the complications of hepatic and prostate cryotherapy. World J Surg 1999; 23:109–113.
24. Lee FT, Littrup PJ, Chosy SG. Minimally invasive alternatives to traditional operative hepatic cryoablation: works in progress. Surg Technol Int 1998; VII:69–78.
25. Matsui K, Amaoka N, Osada S, et al. Percutaneous cryoablation therapy under local anesthesia for unresectable metastatic liver tumors. Gan To Kagaku Ryoho 2003; 30:1591–1594. [Japanese]
26. Dohi M, Harada J, Mogami T, Fukuda K, Toyama Y, Kashiwagi H. MR-guided percutaneous cryotherapy of malignant liver tumor under horizontal-magnetic open system: initial experience. J Hepatobiliary Pancreat Surg 2003; 10:360–365.
27. Goldberg SN, Gazelle GS, Mueller PR. Thermal ablation therapy for focal malignancy: a unified approach to underlying principles, techniques, and diagnostic imaging guidance. AJR Am J Roentgenol 2000; 174:323–331.
28. Saliken JC, Donnelly BJ, Rewcastle JC. The evolution and state of modern technology for prostate cryosurgery. Urology 2002; 60(2 suppl 1):26–33.
29. Chinn SB, Lee FT Jr, Kennedy GD, et al. Effect of vascular occlusion on radiofrequency ablation of the liver: results in a porcine model. AJR Am J Roentgenol 2001; 176:789–795.
30. Cha CH, Lee FT Jr, Gurney JM, et al. CT versus sonography for monitoring radiofrequency ablation in a porcine liver. AJR Am J Roentgenol 2000; 175:705–711.
31. Lee FT Jr, Chosy SG, Littrup PJ, Warner TF, Kuhlman JE, Mahvi DM. CT-monitored percutaneous cryoablation in a pig liver model: pilot study. Radiology 1999; 211:687–692.
32. Weber SM, Lee FT Jr, Chinn DO, Warner T, Chosy SG, Mahvi DM. Perivascular and intralesional tissue necrosis after hepatic cryoablation: results in a porcine model. Surgery 1997; 122:742–747.
33. Goldberg SN, Gazelle GS, Compton CC, Mueller PR, Tanabe KK. Treatment of intrahepatic malignancy with radiofrequency ablation: radiologic-pathologic correlation. Cancer 2000; 88:2452–2463.
34. Littrup PJ, Wang H, Duan Y, Zhang Y, Feng H, Nie Z. Percutaneous cryotherapy of the thorax: clinical observations from more than 200 procedures (abstr). In: Radiological Society of North America scientific assembly and annual meeting program. Oak Brook, Ill: Radiological Society of North America, 2003; 438.
35. Seifert JK, France MP, Zhao J, et al. Large volume hepatic freezing: association with significant release of the cytokines interleukin-6 and tumor necrosis factor α in a rat model. World J Surg 2002; 26:1333–1341.
36. Solbiati L, Ierace T, Tonolini M, Osti V, Cova L. Radiofrequency thermal ablation of hepatic metastases. Eur J Ultrasound 2001; 13:149–158.
37. Solbiati L, Goldberg SN, Ierace T, et al. Hepatic metastases: percutaneous radiofrequency ablation with cooled-tip electrodes. Radiology 1997; 205:367–373.
38. de Baere T, Elias D, Dromain C, et al. Radiofrequency ablation of 100 hepatic metastases with a mean follow-up of more than 1 year. AJR Am J Roentgenol 2000; 175:1619–1625.
39. Rewcastle JC, Sandison GA, Muldrew K, Saliken JC, Donnelly BJ. A model for the time dependent three-dimensional thermal distribution within iceballs surrounding multiple cryoprobes. Med Phys 2001; 28:1125–1137.
40. Weber SM, Lee FT Jr, Warner TF, Chosy SG, Mahvi DM. Hepatic cryoablation: US monitoring of extent of necrosis in normal pig liver. Radiology 1998; 207:73–77.
41. Silverman SG, Tuncali K, Adams DF, et al. MR imaging-guided percutaneous cryotherapy of liver tumors: initial experience. Radiology 2000; 217:657–664.
42. Solbiati L, Ierace T, Goldberg SN, et al. Percutaneous US-guided radio-frequency tissue ablation of liver metastases: treatment and follow-up in 16 patients. Radiology 1997; 202:195–203.
43. Removal of blood from laboratory animals and birds: first report of the BVA/FRAME/RSPCA/UFAW Joint Working Group on Refinement. Lab Anim 1993; 27:1–22.
44. Goldberg SN, Stein MC, Gazelle GS, Sheiman RG, Kruskal JB, Clouse ME. Percutaneous radiofrequency tissue ablation: optimization of pulsed-radiofrequency technique to increase coagulation necrosis. J Vasc Interv Radiol 1999; 10:907–916.
45. McGahan JP, Brock JM, Tesluk H, Gu WZ, Schneider P, Browning PD. Hepatic ablation with use of radio-frequency electrocautery in the animal model. J Vasc Interv Radiol 1992; 3:291–297.
46. Lee FT Jr, Haemmerich D, Wright AS, Mahvi DM, Sampson LA, Webster JG. Multiple probe radiofrequency ablation: pilot study in an animal model. J Vasc Interv Radiol 2003; 14:1437–1442.